Predictive control for the stabilization of a fast mechatronic system : from simulation to real-time experiments

Ahmed Chemori, Nahla Touati

Predictive control for the stabilization of a fast mechatronic system : from simulation to real-time experiments

N. Touati * **A. Chemori** **

* *Research laboratory of automatic LA.R.A, ENIT, BP, 1002 Tunisia (e-mail: nahla.karmani@gmail.com).*
** *LIRMM, Univ. Montpellier 2 - CNRS, 161 rue Ada, 34392 Montpellier, France (e-mail: Ahmed.Chemori@lirmm.fr).*

Abstract: In this paper a Generalized Predictive Control (GPC) scheme is proposed for the stabilization of a fast mechatronic system. Namely the inertia wheel inverted pendulum, which has two degrees of freedom and one actuator. The proposed control approach should be able to stabilize this system around its unstable equilibrium point and maintain it in this state. The efficiency and performance of the proposed control scheme are firstly illustrated through simulation results, then its robustness is shown through real-time experiments on the prototype of the system in question.

Keywords: Generalized Predictive Control, stabilization, mechatronic, inertia wheel inverted pendulum.

1. INTRODUCTION

Mechatronics is the synergistic combination of mechanical engineering, electronics, control systems and computers. The key element in mechatronics is the integration of these areas through the design process as in robotics, digitally controlled combustion engines, automated guided vehicles, etc. Mechatronic systems are generally characterized by significant nonlinearities and input and state constraints. Predictive Control can then be a systematic methodology to handle these challenging control problems (Keerthi and Gilbert 1988, Mayne and Michalska 1990).

Predictive controllers are based on the receding horizon methodology that offers a powerful approach to design state feedback controllers for constrained systems (Mayne, Rawlings, Rao, and Scokaert, 2000). The receding horizon control is a form of control in which the current control action is obtained by solving online, at each sample time, a finite horizon open-loop optimal control problem (Richalet et al., 1978), using the current state of the plant as the initial state; the optimization yields to an optimal control sequence and only the first sample in this sequence is applied. The resolution of the optimization problem, often subject to constraints, becomes difficult in the case of nonlinear systems because of the long computational time. Therefore, the optimization algorithm should have speed and convergence properties (Cannon, 2004) through a set of local and global methods (Horst and Pardalos 1995) to ensure a good control performance. In the case of a linear process model, an analytical solution of the optimization problem without constraints is possible and easy to calculate ; furthermore the control performance may be better since the global optimum can be reached (Cutler, 1979; Clarke, 1987; Flaus, 1994). Consequently, different model predictive control techniques based on this principle can be applied, especially for fast dynamic mechatronic systems.

Generalized predictive control (GPC) is one of these techniques. It provides an analytical solution of the optimization problem (in the absence of constraints). This control scheme can deal with unstable as well as non-minimum phase systems. It is one of the most popular approaches of Model Predictive Control (MPC) both in industry and academia.

In this paper we discuss this control approach for the problem of stabilization of a nonlinear fast mechatronic system, namely the inertia wheel inverted pendulum [16].

The inverted pendulum system is a standard problem in the area of control systems. It is often used to demonstrate concepts in linear and nonlinear control such as stabilization or swinging up of unstable systems. This system belongs to the class of non-minimum systems because of its unstable internal dynamics. One interesting example of inverted pendulum is the inertia wheel inverted pendulum; it is underactuated system since the number of its control inputs is less than the number of its degrees of freedom, which makes it difficult to control. In this paper, the aim of the proposed control scheme (GPC) is to stabilize the inertia wheel inverted pendulum around its unstable equilibrium point and to maintain it in this state, even if it is subject to external disturbances, or in the presence of parametric uncertainties. Numerical simulations as well as real-time experiments are presented to show the effectiveness of the proposed control scheme and its robustness towards external disturbances and changes in system dynamics.

This paper is organized as follows. In section 2, the inertia wheel inverted pendulum is described and its dynamic model is given. The generalized predictive control law is presented in section 3. Section 4 is dedicated to simulation results, while experiments are presented and discussed in section 5. Finally, concluding remarks are drawn in section 6.

2. DESCRIPTION AND DYNAMICS OF THE MECHATRONIC SYSTEM

2.1 Description of the system

The inertia wheel inverted pendulum system (shown in Fig. 1) consists of three main parts : the mechanical part, the computer and the electronic part.

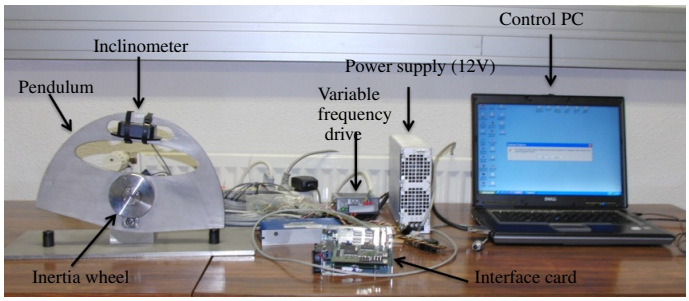

Fig. 1. Inertia wheel inverted pendulum system

Description of the mechanical part of the system
The underactuated mechanical system studied in this paper is the inertia wheel inverted pendulum (cf. Fig. 2), which consists of an inverted pendulum equipped with a rotating wheel. The joint between the the pendulum body and the frame is unactuated; whereas the joint between the beam and the wheel is actuated by a Maxon EC-powermax 30 DC motor (cf. Fig. 3). The schematic representation of the inertia wheel inverted pendulum is depicted in Fig. 6. The motor torque produces an angular acceleration of the rotating wheel which generates, thanks to the dynamic coupling between coordinates, a torque acting on the pendulum's passive joint; therefore this last one can be controlled through the acceleration of the inertia wheel.

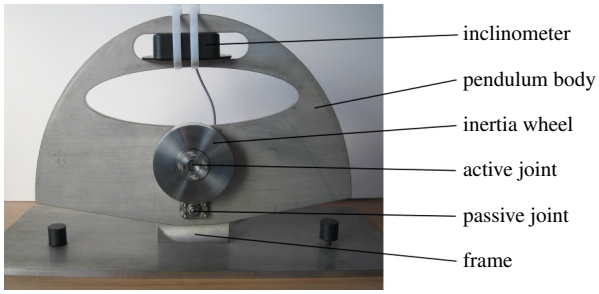

Fig. 2. Mechanical part of the system

Fig. 3. Maxon EC-powermax 30 DC motor

Description of the computer and electronic parts of the system
The actuator of the system is a Maxon EC-powermax 30 DC motor, equipped with an incremental encoder as shown in Fig. 4 , allowing the measurement in real-time of the inertia wheel angular position.

In order to measure the angular position of the pendulum

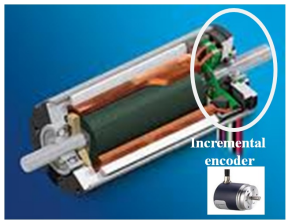

Fig. 4. The DC motor equipped with an incremental encoder

with respect to the vertical, the system is equipped with an inclinometer FAS-G of Micro strain (cf. Fig. 5). The system is controlled with a computer equipped with a 2.4 GHz Intel processor. The control approach is implemented using C++ language, and the whole system is running under Ardence RTX real-time OS.

Fig. 5. inclinometer FAS-G of Micro strain

2.2 Dynamic modeling of the system

The nonlinear dynamic model of the system (12) is obtained using Lagrange formulation [8], and is given by:

$$\begin{bmatrix} I+i_2 & i_2 \\ i_2 & i_2 \end{bmatrix} \begin{bmatrix} \ddot{\theta}_1 \\ \ddot{\theta}_2 \end{bmatrix} + \begin{bmatrix} -\overline{ml}g\sin\theta_1 \\ 0 \end{bmatrix} = \begin{bmatrix} C_1 \\ C_2 \end{bmatrix} \qquad (1)$$

where:

- θ_1 and θ_2 are, respectively, the angular positions of the pendulum body and the inertia wheel (cf. Fig. 6);
- $\dot{\theta}_i$ and $\ddot{\theta}_i$ $(i = 1,2)$, represent their corresponding velocities and accelerations;
- C_1 is the external disturbing torque applied on the pendulum (in this study, it is supposed nul);
- C_2 is the torque generated by the system's actuator;
- i_1, i_2 are respectively the moments of inertia of the pendulum body and the wheel;
- $I = m_1 {l_1}^2 + m_2 {l_2}^2 + i_1$ with m_1 and m_2 being the masses of the pendulum and the inertia wheel. l_1 and l_2 are the distances from the origin O (cf. Fig. 6) to the gravity centers of the pendulum and the rotating mass (respectively);
- and $\overline{ml} = m_1 l_1 + m_2 l_2$.

2.3 State space representation of the model

The state space representation of the inertia wheel inverted pendulum is obtained through linearization of the nonlinear dynamic model presented above around the unstable equilibrium point. Let the state vector x_c be defined as: $x_c = [\,\theta_1\ \dot{\theta}_1\ \dot{\theta}_2\,]^T$ and $u = C_2$. The unstable equilibrium point (x_c^*, u^*) is defined

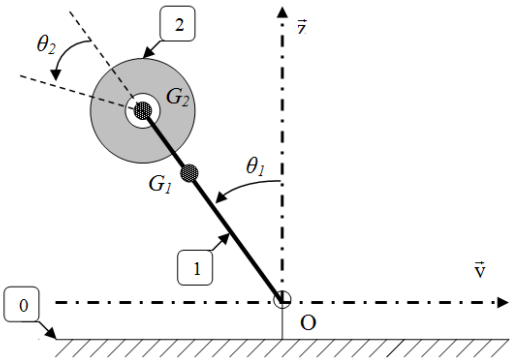

Fig. 6. Schematic view of the inertia wheel inverted pendulum

as : $(x_c^* = [\,0\;0\;0\,]^T, u^* = 0)$.
The linear state space representation of the inertia wheel inverted pendulum is given by the following equations :

$$\begin{cases} \dot{x}_c = A_c x_c + B_c u \\ y_c = C_c x_c + D_c u \end{cases} \tag{2}$$

where:

$$A_c = \begin{bmatrix} 0 & 1 & 0 \\ \overline{ml}g/I & 0 & 0 \\ -\overline{ml}g/I & 0 & 0 \end{bmatrix},\; B_c = \begin{bmatrix} 0 \\ -1/I \\ (i_2+I)/I/ \end{bmatrix},$$

$C_c = [\,1\;0\;0\,]$ and $D_c = [\,0\,]$

3. PROPOSED APPROACH: GENERALIZED PREDICTIVE CONTROL (GPC)

The goal of the proposed approach is to stabilize the inertia wheel inverted pendulum around its unstable equilibrium point; and to maintain it in this state even if it is subject to external disturbances, or in the presence of parametric uncertainties.

3.1 Model representation for the GPC

The control design requires a discrete state space representation. Let's consider the state vector x_d defined by: $x_d = [\,\theta_1(k)\;\dot{\theta}_1(k)\;\dot{\theta}_2(k)\,]^T$. The discretization of the state space dynamics (2) leads to following discrete time representation:

$$\begin{cases} x_d(k+1) = A_d x_d(k) + B_d u(k) \\ y_d(k) = C_d x(k) + D_d u(k) \end{cases} \tag{3}$$

where:

$A_d = e^{A_c T}$, $B_d = \int_0^T e^{A_c(T-\tau)} B_c \tau$, $C_d = C_c$ and $D_d = D_c$.
where A_c, B_c, C_c and D_c are the matrices of the continuous state space representation and T is the sampling period.

Let's now consider the control input increment at instant k: $\Delta u(k) = u(k) - u(k-1)$ and the extended space vector $x_e = \begin{bmatrix} x_d(k+1) \\ u(k) \end{bmatrix}$, the system dynamics can then be rewritten as follows:

$$\begin{cases} x_e(k+1) = A_e x_e(k) + B_d \Delta u(k) \\ y_e(k) = C_e x_e(k) + D_e \Delta u(k) \end{cases} \tag{4}$$

where:

$$A_e = \begin{bmatrix} A_d & B_d \\ 0 & 1 \end{bmatrix},\; B_e = \begin{bmatrix} B_d \\ 1 \end{bmatrix},\; C_e = [C_d \;\; 0] \text{ and } D_e = D_d.$$

For the rest of the paper, consider the following notation : $x = x_e$, $A = A_e$, $B = B_e$, $C = C_e$ and $y = y_e$.

3.2 GPC basic principle

The Generalized Predictive Control (GPC) scheme was initially proposed by Clarke et al [17] and has become one of the most popular Model Predictive Control (MPC) schemas both in industry and academia. The basic idea of GPC is to compute a future control sequence such it minimizes a multiobjective cost function defined over a prediction horizon. The performance index to be optimized is a quadratic function including a term measuring the distance between the predicted system output and the reference sequence over the horizon plus a term measuring the control effort.
GPC has many ideas in common with the other model predictive controllers since it is based upon the same concepts; nevertheless, it has also some differences. It provides an analytical solution (in the absence of constraints), it can deal with unstable and non-minimum phase systems and incorporates the concept of receding horizon as well as the consideration of weighting of control increments in the cost function.
The proposed GPC formulation should involve all the states of the system, and introduce a penalty condition on the final state. Indeed, the classical formulation of the GPC with a transfer function as input / output model of the system does not guarantee the control of all system states. This is because such a model involves only the outputs of the system and not all the states.
In the case of our system, the objective is to impose : $\theta_1(t_f) = \dot{\theta}_1(t_f) = \ddot{\theta}_2(t_f) = 0$ where t_f characterizes the end of the prediction horizon at each sampling instant.
For this formulation, the cost function J to be minimized is as follows:

$$\begin{aligned} J = & \sum_{j=N_1}^{N_p} (y(k+j) - w(k+j))^T (y(k+j) - w(k+j)) \\ & + (x(k+N_p) - w_x(k+N_p))^T Q (x(k+N_p) - w_x(k+N_p)) \\ & + \sum_{j=1}^{N_u} \lambda(j) (\Delta u(k+j-1))^T (\Delta u(k+j-1)) \end{aligned} \tag{5}$$

where: N_1 and N_p are the beginning and the end prediction horizons, N_u is the length of the control horizon, Q and λ are the weights on the states and the control respectively and w_x is the desired final state of the system.
The calculation of the cost function requires the prediction of future outputs $y(k+j)$, $j = 1 \ldots N_p$ at each sampling instant k based on the information available on the system at previous times. From the state space representation of the system, we have:

$$\begin{aligned} x(k+1) &= Ax(k) + B\Delta u(k) \\ x(k+2) &= Ax(k+1) + B\Delta u(k+1) = A^2 x(k) + Bu(k+1) \\ &\vdots \\ x(k+j) &= A^j x(k) + \sum_{i=0}^{j-1} A^{j-i-1} B \Delta u(k+i) \end{aligned} \tag{6}$$

Therefore, the estimated output of the system at time $k+j$ is written as:

$$y(k+j) = CA^j x(k) + \sum_{i=0}^{j-1} CA^{j-i-1} B \Delta u(k+i) \tag{7}$$

Since the control horizon is shorter that the prediction horizon $N_u \leq N_p : \forall i \geq N_u$, $u(k+i) = 0$, and if we consider:

$$y = \begin{bmatrix} y(k+1) \\ y(k+2) \\ \vdots \\ y(k+N_1) \\ \vdots \\ y(k+N_p) \end{bmatrix} \quad , \quad \Delta u = \begin{bmatrix} \Delta u(k) \\ \Delta u(k+1) \\ \Delta u(k+2) \\ \vdots \\ \Delta u(k+N_u) \end{bmatrix} \tag{8}$$

Then the predicted output can be rewritten in matrix form as follows:

$$y = G\Delta u + f \tag{9}$$

where G and f are given by:

$$G = \begin{bmatrix} CB & 0 & 0 & \dots & 0 \\ CAB & CB & 0 & \dots & 0 \\ \vdots & \vdots & \vdots & \dots & \vdots \\ CA^{N_1-1}B & CA^{N_1-2}B & CA^{N_1-3}B & \dots & 0 \\ \vdots & \vdots & \vdots & \dots & \vdots \\ CA^{N_p-1}B & CA^{N_p-2}B & CA^{N_p-3}B & \dots & CA^{N_p-N_u}B \end{bmatrix}$$

and $f = \begin{bmatrix} CA \\ CA^2 \\ \vdots \\ CA^{N_1} \\ \vdots \\ CA^{N_p} \end{bmatrix} x(k).$

The control sequence should be derived from the criterion (5). Since we are interested on the stabilization problem, let's consider : $w_x = 0, w(k+j) = 0 \quad \forall j, N_1 = 1, N_p = N_u = N$, $Q \geq 0$ et $\lambda(j) = \lambda > 0$.
The criterion (5) can then be rewritten as follows:

$$J_N = \sum_{j=1}^{N} y(k+j)^T y(k+j) + \lambda \Delta u(k+j-1)^T \Delta u(k+j-1) + x^T(k+N)(Q+C^T C)x(k+N) \tag{10}$$

The state of the system at time $k+N$ is given by:

$$x(k+N) = A^N x(k) + \bar{C}\Delta u \tag{11}$$

Where: $\bar{C} = [A^{N-1}B \quad A^{N-2}B \ \dots \ B]$.
The cost function can then be reformulated as follows:

$$J_N = \frac{1}{2}[H + 2\bar{C}^T Q\bar{C}]\Delta u + [b + 2x^T(k)(A^N)^T Q\bar{C}]\Delta u + f_0 + x^T(k)(A^N)^T Q A^N x(k) \tag{12}$$

Where:

- $H = 2[G^T G + \lambda I]$;
- $b = 2f^T G$;
- $f_0 = f^T f$.

The optimal control sequence that minimizes the performance index (12) is obtained from the solution of the equation $\frac{\delta J_N}{\delta \Delta u} = 0$. The obtained optimal solution Δu^* is then written as follows:

$$\Delta u^* = -Kx(k) \tag{13}$$

Where:

$$K = (G^T G + \lambda I + \bar{C}^T Q\bar{C})^{-1}(G^T L + \bar{C}^T Q A^N)$$

It is worth to note, according to the basic principle of predictive control, that only the first sample of the optimal control sequence is applied to the controlled system.

4. SIMULATION RESULTS

Simulation results, obtained using Matlab software, are presented and discussed in this section. As a first validation, they show the feasibility of the proposed control scheme. One simulation scenario is considered to validate the robustness of the proposed control scheme. The first scenario is to consider the system in the nominal case without any external disturbances. While the second one aims to show the robustness of the controller against parameter's uncertainties.

4.1 Scenario 1: Stabilization in the nominal case

Consider the dynamic model of system (1) with physical parameters summarized in Table 1. These parameters have been identified on the real prototype of the system described in section 2.

Table 1. Description of dynamic parameters of the system

Parameter	Description	Value	unit
m_1	Body mass	3.30810	Kg
m_2	Wheel mass	3.33081	Kg
l_1	Body center of mass position	0.06	m
l_2	Wheel center of mass position	0.044	m
i_1	Body inertia	0.0314683	Kgm^2
i_2	Wheel inertia	0.0004176	Kgm^2

The proposed simulation is started from the initial condition $x_0 = [\theta_1 = 18^\circ \ \ \dot{\theta}_1 = 0 \ \ \dot{\theta}_2 = 0]^T$. Table 2 describes the parameters of the proposed control scheme.

Table 2. Description of the control parameters

Parameter	Description	Value
N_1	Minimum prediction horizon	40
N_p	Maximum prediction horizon	40
N_u	Length of control horizon	40
λ	Control weight	40
Q	State weight	$I_d(3,3)$

Fig. 7 displays the obtained simulation results for the nominal case. Fig. 7-(a) and 7-(b) show the evolution of the pendulum body joint position and velocity. The inertia wheel velocity versus time is displayed in Fig. 7-(c). Fig. 7-(d) represents the control input that consists of the motor voltage (proportional to the motor torque).
From the obtained results, it can be observed that the controller is able to stabilize the system around its unstable equilibrium point and keep it around this position.

4.2 Scenario 2: Robustness towards parameter's uncertainties

The test of the proposed controller robustness allows us to check whether the applied control is capable of compensating the uncertainties on the system parameters. These uncertainties were not considered in the modeling phase of the system.
Let's now consider the case of an uncertainty on the parameter inertia I that is:

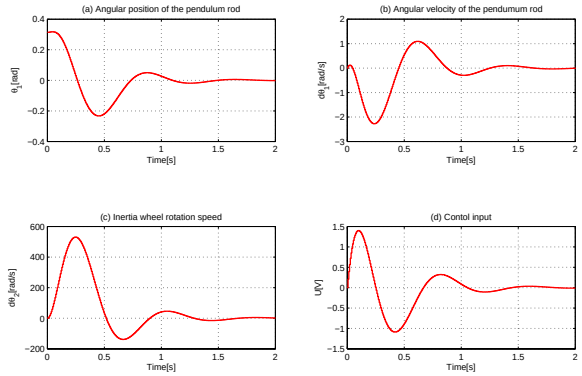

Fig. 7. Simulation result in the nominal case

$$I^{'} = I + \Delta I \times I \tag{14}$$

Three cases are considered : the nominal case corresponding to $\Delta I = 0\%$, and two other cases corresponding to an uncertainty of $\Delta I = 10\%$ and 45%, respectively. The objective would then be to see if the proposed controller is able to compensate this uncertainty. Fig. 8 displays the evolution of the system states in these three cases. We notice clearly the ability of the GPC controller to ensure system stabilization despite the misidentification introduced that can go up to 45% uncertainty on the parameter I. Note also that the system is becoming slightly slower when increasing the uncertainty amount.

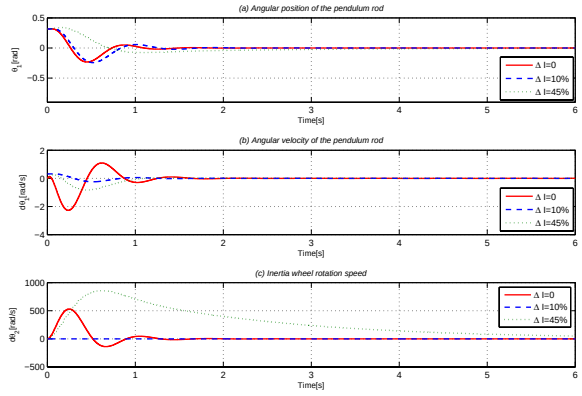

Fig. 8. Robustness towards uncertainties

5. REAL-TIME EXPERIMENTAL RESULTS

In this section the obtained real-time experimental results are presented and discussed. They are performed on the inverted pendulum testbed presented in section 2. Two experimental scenarios are studied. In the first one the proposed control scheme is implemented without considering any external disturbance, whereas in the second one, to show its effectiveness, the system is subject to external disturbances.

5.1 Scenario 1: Stabilization without external disturbances

The controller design parameters used for this experiment are the same as those used in simulation. Fig. 9 shows the overall obtained results of this first scenario. The pendulum joint position and velocity are displayed in Fig. 9-(a) and 9-(b), respectively. Measurement noise can be observed on the pendulum body velocity $\dot{\theta}_1$ since this last one is computed using a numerical derivation of the measured angular position θ_1. Fig. 9-(c) displays the motor velocity versus time. The DC motor input voltage can be observed in Fig. 9-(d). This experiment shows that the controller is able to stabilize the system and keep it around its unstable equilibrium point.

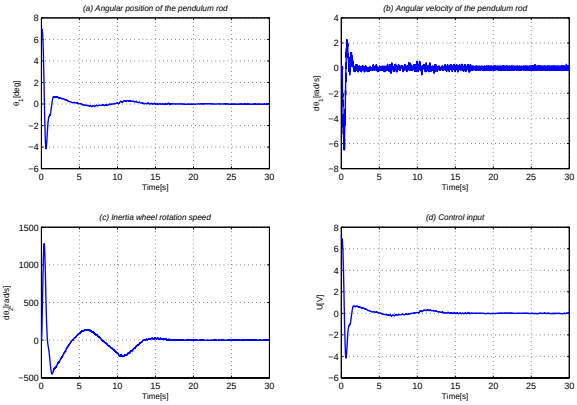

Fig. 9. Experimental results (without external disturbances)

5.2 Scenario 2: Stabilization with external disturbances

In this scenario, two combined types of disturbances were applied on the inverted pendulum. The first one illustrated in Fig.10, consists in pushing the pendulum, which generates external punctual torques applied to the pendulum joint at approximately $t = 8s$, $t = 12s$, $t = 17s$ and $t = 26s$. And the second type of disturbances illustrated in Fig.11 is persistent and applied constantly to the inverted pendulum as an additional mass attached to the pendulum body. The punctual and persistent disturbances can be represented by external forces F_{1ext} and F_{2ext} applied on the inverted pendulum. These forces generate torques τ_{1ext} and τ_{2ext} around the pendulum pivot. These torques, to be compensated, produce a change in the angular velocity of the rotating wheel.

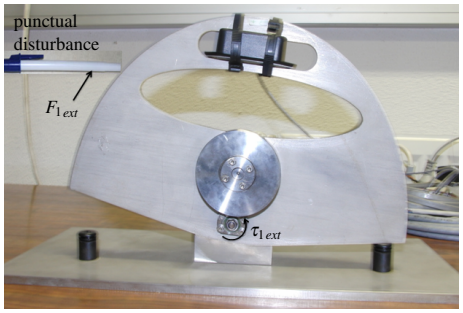

Fig. 10. Punctual disturbance applied on the pendulum

Fig. 12 displays the obtained experimental results for this second scenario. In Fig. 12-(a), the pendulum joint position is displayed. Fig. 12-(b) shows the pendulum joint velocity . External disturbance compensation can be observed in Fig. 12-(c) and 12-(d) where, respectively, the inertia wheel velocity and motor input voltage are displayed. The effect of the punctual

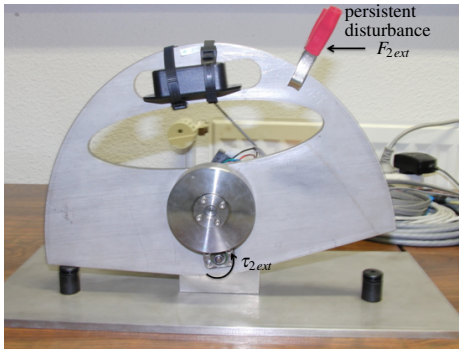

Fig. 11. Persistent disturbance applied on the pendulum

disturbances can be observed as peaks on the curves that appear at instants of application of the disturbing torques. The proposed controller is capable of compensating these disturbances. Besides it succeeds also to compensate the value of the persistent disturbance and to keep the system around its unstable equilibrium position. This fact results in the permanent rotation of the inertia wheel.
Despite the combination of both types of disturbances, the controller is still able to compensate them and maintain the system around its equilibrium point.

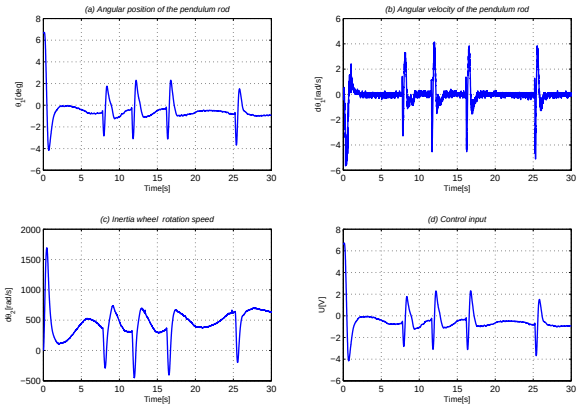

Fig. 12. Experiment results (with external disturbances)

6. CONCLUSION AND FUTURE WORK

In this paper, a Generalized Predictive Controller (GPC) is proposed for stabilization of a fast underactuated mechatronic system. Namely the inertia wheel inverted pendulum. Numerical simulations as well as real-time experiments show the performance and the effectiveness of the proposed control scheme and its robustness towards uncertainties and external disturbances (both punctual and persistent). Our future work will be focused on the generation of stable limit cycles for the inertia wheel inverted pendulum.

REFERENCES

[1] A. Chemori and M. Alamir. Nonlinear predictive control of under-actuated mechanical systems, application: the ECP 505 inverted pendulum. In MTNS'06 Proc. Mathematical Theory of Networks and Systems, Leven, Belgium, 2004.

[2] Bruno Garabedian. Etude de faisabilit d'un tramway monorail. Master's thesis, Master STPI EEA 1ere anne, Universit Montpellier II, September 2006.

[3] J.M.Maciejowski. Predictive control with constraints. Number 346. Pearson Education,2000.

[4] H. Khalil. Nonlinear Systems. Prentice Hall, Upper Saddle River, Second Edition, NJ, USA,1996.

[5] I. Fantoni and R. Lozano. Non-linear control for underactuated mechanical systems. Springer-Verlag, New York, USA, 2001.

[6] M. Reyhanoglu, S. Ludvigsen, and O. Egeland. Discontinuous feedback control of a special class of underactuated mechanical systems. Int. J. Robust and Nonlinear Control, 10(4):265-282, 2000.

[7] M. Spong. Energy based control of a class of underactuated mechanical system. In 13th IFAC World Congress, pages 431-436, San Francisco, USA, 1996.

[8] M. Spong and M. Vidyasagar. Robot Dynamics and Control. John Wiley and Sons, New York, USA, 1989.

[9] M. Spong. Underactuated mechanical systems. Control Problems in Robotics and Automation, B. Siciliano and K. P. Valavanis Eds., LNCIS, Springer Verlag, 230:135-150, 1998.

[10] R. Ginhoux. Compensation des mouvements physiologiques en chirurgie robotise par commande prdictive. Doctoral thesis, Louis Pasteur StarsbourgI University, 2003.

[11] R. Sivan H. Kwakernaak. Linear Optimal Control Systems. Wiley-Interscience, 1972.

[12] S. Andary, A. Chemori, and S. Krut. Control of the underactuated inertia wheel inverted pendulum for stable limit cycle generation. RSJ Adanced Robotics, 23(15):1999-2014, 2009.

[13] S. Andary, A. Chemori, and S. Krut. Estimation-based disturbance rejection in control for limit cycle generation on inertia wheel inverted pendulum testbed. In IEEE/RSJ International Conference on Intelligent RObots and Systems, IROS'09, St-Louis, MO, USA, 2009.

[14] S. Andary, A. Chemori, and S. Krut. Stable limit cycle generation for underactuated mechanical systems, application: Inertia wheel inverted pendulum. In IEEE/RSJ International Conference on Intelligent Robots and Systems, IROS'08, Nice, France, 2008.

[15] V. Coverstone-Carroll K. Lee. Control algorithms for stabilizing underactuated robots. Journal of Robotic Systems, 15(12):681-697, 1998.

[16] M. Spong, P. Corke, and R. Lozano. Nonlinear control of the inertia wheel pendulum. Automatica, 37:1845-1851, 1999.

[17] D. W. Clarke, C. Mohtadi and P. S. Tuffs, Generalized predictive control-part I. the basic algorithm, Automatica, vol 23, pp. 137-148, 1987.